

Supporting Information

A Bottom-up Synthesis of Rare-Earth-Hydroxalate Monolayer Nanosheets toward Multimode Imaging and Synergetic Therapy

Xuan Mei, Jialing Ma, Xue Bai, Xin Zhang, Shaomin Zhang, Ruizheng Liang,*

Min Wei,* David G. Evans, and Xue Duan

State Key Laboratory of Chemical Resource Engineering, Beijing Advanced Innovation
Center for Soft Matter Science and Engineering, Beijing University of Chemical Technology,
Beijing 100029, P. R. China

Correspondence and requests for materials should be addressed to R. L (email:
liangruizheng2000@163.com); M. W. (email: weimin@mail.buct.edu.cn).

Materials and Methods

Materials. All of the chemicals were of analytical-grade and obtained from commercial sources, which were used without any further purification. Magnesium nitrate ($\text{Mg}(\text{NO}_3)_2 \cdot 6\text{H}_2\text{O}$), aluminium nitrate ($\text{Al}(\text{NO}_3)_3 \cdot 9\text{H}_2\text{O}$), gadolinium(III) nitrate ($\text{Gd}(\text{NO}_3)_3 \cdot 6\text{H}_2\text{O}$), ytterbium(III) nitrate pentahydrate ($\text{Yb}(\text{NO}_3)_3 \cdot 5\text{H}_2\text{O}$), sodium hydroxide (NaOH), sodium nitrate (NaNO_3), formamide, ammonia solution ($\text{NH}_3 \cdot \text{H}_2\text{O}$), indocyanine green (ICG) and 7-ethyl-10-hydroxy-camptothecin (SN38) were obtained from Aladdin Chemical. Co. Ltd (Shanghai, China). Calceinacetoxymethyl ester (Calcein-AM) and propidium iodide (PI) were purchased from Sigma-Aldrich Company (St. Louis, MO, USA). High glucose Dulbecco's modified Eagles medium (DMEM), 0.25% trypsin-EDTA and penicillin/streptomycin were obtained from Gibco (Invitrogen, Carlsbad, CA). Fetal bovine serum (FBS) was purchased from Excell Bio. Co., Ltd. (Shanghai, China). Hoechst 33342, phosphate-buffered saline (PBS) and Annexin V-FITC & propidium iodide apoptosis detection kit were purchased from Solarbio Science & Technology Co, Ltd (Beijing, China). Ultrapure water from a Milli-Q Millipore system was used in all the processes.

Synthesis of Gd&Yb-LDH monolayer nanosheets. Firstly, $\text{Mg}(\text{NO}_3)_2 \cdot 6\text{H}_2\text{O}$ (0.768 g), $\text{Al}(\text{NO}_3)_3 \cdot 9\text{H}_2\text{O}$ (0.450 g), $\text{Gd}(\text{NO}_3)_3 \cdot 6\text{H}_2\text{O}$ (0.045 g) and $\text{Yb}(\text{NO}_3)_3 \cdot 5\text{H}_2\text{O}$ (0.045 g) were dissolved in a mixed solvent containing 47.5 mL of deionized water and 20 mL of formamide. After stirring for 10 min, 2.5 mL of ammonia solution was added dropwise, and the mixture was sealed in a Teflon-lined stainless-steel autoclave and heated at 110 °C for 30 min. After washing with deionized water and ethanol thoroughly *via* centrifugation, the resulting precipitation was re-dispersed in water and centrifugated again at a rate of 4000 rpm to obtain

Gd&Yb-LDH monolayer nanosheets in the supernatant. Furthermore, a dialyzed treatment (8 kDa) was carried out to remove residual formamide.

T₁-weighted MRI study. MRI was performed on small animal MRI instrument in the field of 7.0 T (BioSpin, BRUKER, Germany). T₁-weighted MR images of Gd&Yb-LDH were measured with different Gd concentrations of 0, 0.005, 0.01, 0.02, 0.04 mM, respectively. The parameters of T₁ RARE sequence used here were as follows: TR= 300 ms, TE= 6.06 ms, field of view= 45 mm×45 mm, matrix size= 256×256, number of slices= 20, slice thickness= 1 mm, flip angle= 90 °and NEX= 2.

Drug loading. Firstly, 10 mg of SN38 was dissolved in dimethyl sulfoxide (DMSO, 10 mL) to obtain the stock solution. For the preparation of SN38/Gd&Yb-LDH with various mass ratios, SN38 stock solution was added into Gd&Yb-LDH (1 mg/mL) suspension with mass ratio from 1: 1 to 10: 1. After stirring for 3 h, SN38/Gd&Yb-LDH was centrifuged at 10000 rpm for 5 min, collected and re-dispersed thoroughly in DI-water. Such progress was repeated for 4 times to remove excess SN38 and DMSO, after which the sample was re-dispersed in water for further use. The preparation procedure of ICG/Gd&Yb-LDH was similar to SN38/Gd&Yb-LDH by using deionized water as a solvent instead of DMSO. Typically, in the preparation of SN38&ICG/Gd&Yb-LDH, SN38 and ICG were mixed, added to Gd&Yb-LDH suspension and then stirred for 3h, followed by the same centrifugation process.

Determination of loading content (LC) and encapsulation efficiency (EE). The drug concentration in the initial solution and supernatant was determined according to the UV-vis absorbance at 370 nm for SN38 and 780 nm for ICG. The LC and EE of SN38, ICG and

SN38&ICG were calculated by the equations below:

$$LC-1 = (W_{Fed} - W_{Non-encapsulated}) / W_{Gd\&Yb-LDH} \times 100\% \quad (1)$$

$$LC-2 = (W_{Fed} - W_{Non-encapsulated}) / W_{total} \times 100\% \quad (2)$$

$$EE = (W_{Fed} - W_{Non-encapsulated}) / W_{Fed} \times 100\% \quad (3)$$

Where W_{Fed} represents the initial total mass of added drug; $W_{Non-encapsulated}$ is the unencapsulated drug mass in supernatant after centrifugation; $W_{Gd\&Yb-LDH}$ represents the total mass of added Gd&Yb-LDH during the drug loading; W_{total} represents the total mass of added Gd&Yb-LDH and encapsulated drug.

Isothermal titration calorimetry (ITC) measurements. ITC measurements were performed on a Nano ITC (TA Instruments Waters, LLC, UT) in the following procedure: 250 μ L of ICG (1.0×10^{-3} mol/L) suspension was added dropwise through a calorimeter injection syringe into 1.2 mL of SN38 (1.0×10^{-4} mol/L) stored in ITC cell at 25 $^{\circ}$ C. A full heat equilibration was maintained by setting the titration gap at 300 s. An independent model was performed to obtain titration curves; the thermodynamic parameters (enthalpy change ΔH , entropy change ΔS and affinity constant K_A) were obtained by TA Instruments NanoAnalyzeTM software. The measurement between SN38&ICG (1.0×10^{-4} mol/L) and Gd&Yb-LDH aqueous suspension (1.0×10^{-3} mol/L) was carried out in the same process.

Photothermal effect of SN38&ICG/Gd&Yb-LDH. To detect the temperature variation, 1.0 mL of SN38&ICG/Gd&Yb-LDH (2.5 μ g/mL), ICG (2.5 μ g/mL), and PBS were placed in a 1.5 mL of glass vial, respectively. The temperature change was monitored using a thermal infrared imaging camera (Fluke Ti450, USA) with NIR laser irradiation (808 nm fiber-coupled semiconductor diode, 1 W/cm²) at the bottom of vial. At the same time, thermal

infrared images were recorded at different time points. The photothermal performance under other conditions was carried out by the same method.

pH and photo-stimulated release of SN38 from SN38&ICG/Gd&Yb-LDH. The pH of SN38&ICG/Gd&Yb-LDH (2.5 $\mu\text{g}/\text{mL}$) suspension was adjusted to 5.5, 6.5 and 7.4, respectively, followed by continues irradiation (808 nm, 1.0 W/cm^2) for 3 min. The released SN38 in the supernatant was separated by centrifugation and quantified *via* UV-vis absorption at 370 nm. The fluorescence spectra and photographs under UV irradiation were recorded as well.

Detection of singlet oxygen production. 1,3-diphenylisobenzofuran (DPBF) was used as a probe to detect singlet oxygen production. Briefly, A DPBF acetonitrile solution (20 μL , 70 μM) was added into 2 mL of ICG or SN38&ICG/LDH suspension (ICG equivalent concentration: 2.5 $\mu\text{g}/\text{ml}$), respectively. The mixed suspension was irradiated by an 808 nm laser irradiation (1.0 W/cm^2) for 8 min and the UV-vis absorption spectra were monitored every minute. The singlet oxygen production efficiency is proportional to the decrease rate of DPBF absorption intensity at 410 nm.

Cell line and culture. Hela cells were obtained from Institute of Basic Medical Sciences Chinese Academy of Medical Sciences (Beijing, China). Cells were incubated in a 25 cm^2 cell-culture flask and cultured well in Dulbecco's modified Eagle's medium (DMEM) containing 10% fetal bovine serum (FBS) and 1% penicillin-streptomycin in an atmosphere of 5% CO_2 at 37 $^\circ\text{C}$. After cells spread over 80% of the bottom, 1.0 mL of trypsin (0.25%) was added to detach cells (2–3 min) followed by adding 2 mL of DMEM to terminate digestion.

***In vitro* fluorescence image.** HeLa cells were trypsinized and expanded on confocal dishes (35 mm) in an incubator for 24 h (37 °C; 5% CO₂). Afterwards, cells were incubated with SN38&ICG/Gd&Yb-LDH suspension (5 µg/mL, 2 mL) for 6 h. After incubation, the cells were washed thoroughly with sterile PBS for 3 times, and Hoechst 33342 (10 µg/mL, 2 mL) was added to stain nuclei of cells. After 10 min, cells were washed with PBS again for 3 times. Finally, images were obtained using a Leica confocal laser scanning microscopy (Leica, Germany).

***In vitro* MTT assay and the cell death mode monitoring.** The cells were suspended in two 96-well plates with a concentration of 1×10⁴ cells/well and cultured at 37 °C with 5% CO₂ for 24 h. Afterwards, cells were incubated with 100 µL of medium containing various samples including PBS, Gd&Yb-LDH, SN38, ICG, SN38&ICG, SN38/Gd&Yb-LDH, ICG/Gd&Yb-LDH and SN38&ICG/Gd&Yb-LDH, respectively, with a series concentration from 0.2 to 5 µg/mL for another 24 h. Then, cells were washed with PBS thoroughly for 3 times, and one plate was irradiated by 808 nm laser (1.0 W/cm²) for 3 min while another was kept for dark toxicity study. Afterwards, both of the plates were placed in an incubator for another 6 h followed by the standard methyl thiazolyl tetrazolium (MTT) assay. Cell viability was calculated by the following equation:

$$\text{Cell viability} = \text{OD } 490 \text{ nm}_{\text{the experimental group}} / \text{OD } 490 \text{ nm}_{\text{the control group}} \times 100\% \quad (4)$$

In addition, cells were stained with Calcein-AM/PI to visualize the population of viable and necrotic cells. The mode of cell death was determined using an annexin V-FITC and PI staining kit according to the manufacturer's instructions.

Calculation of combination index (CI). In a certain drug combination, CI is usually

calculated to evaluate the synergetic effect of drugs. In this work, the synergistic effect in this chemo/PTT/PDT tri-mode therapy was achieved through the combination of SN38 and ICG, so CI value was used to reveal the effect of tri-mode therapy compared with the sum of each treatment. CI is calculated by the following formula:¹

$$CI = D_1 / D_{m1} + D_2 / D_{m2} \quad (5)$$

where D_1 and D_2 are the concentrations of drug 1 and drug 2 that in combination to produce certain amount of cell inhibition (*e.g.*, 50%); while D_{m1} and D_{m2} represent the concentrations of these drugs administered alone to induce the same cellular cytotoxicity. CI value significantly lower than 1.0 indicates synergism; CI value higher than 1.0 represents antagonism; CI value equal to 1.0 represents additivity.²

Animal experiments. Male Balb/c mice (Balb/c-nude, aging 4–6 weeks) were purchased from Beijing Vital River Laboratory Animal Technology Co., Ltd and maintained in a 12 h/12 h light/dark cycle controlled environment. The animal procedures followed the protocols approved by China-Japan friendship Hospital Animal Research Center. To establish the tumor models, mice were subcutaneously inoculated with 1×10^7 Hela cells suspended in 100 μ L of PBS in the position of right back. All the experiments were performed when the tumor volume reached 70 mm³.

***In vivo* MRI and CT study.** To investigate *in vivo* MRI and CT imaging, mice were injected intravenously with SN38&ICG/Gd&Yb-LDH (200 μ L, 5.6 mM of Gd and Yb). MR images were obtained using T₁ RARE sequence with the following parameters: TR= 500 ms, TE= 9 ms, field of view= 3 cm×3 cm, matrix size= 256×256, number of slices= 20, slice thickness= 1 mm, flip angle= 180° and NEX= 4. *In vivo* CT imaging was performed on a SIEMENS

Inveon device (Germany) with the parameters: tube voltage 80 kV, tube current 500 μ A, rotation time 280 ms, CCD: 2048 \times 3072. The same parameters were used in the CT value determination.

***In vivo* fluorescence imaging.** PBS, SN38&ICG/Gd&Yb-LDH, and SN38&ICG (200 μ L, ICG concentration of 1 mg/kg) were intravenously injected into the tumor-bearing mice, respectively. The fluorescent images at 0 h, 2 h, 6 h, 12 h and 24 h (excitation: 780 nm; emission: 831 nm) were acquired on an IVIS lumina fluorescence imaging system. All the images were obtained with the same parameter settings and scale.

***In vivo* antitumor therapy.** Mice were randomized into eight groups (6 animals per group) and injected intravenously with different samples: (Group 1) PBS (200 μ L) without irradiation; (Group 2) Gd&Yb-LDH (200 μ L, 3 mg/kg) without irradiation; (Group 3) SN38&ICG (200 μ L, 3 mg/kg for the total dose of SN38 and ICG) without irradiation; (Group 4) SN38&ICG/Gd&Yb-LDH (200 μ L, 3 mg/kg for the total dose of SN38 and ICG) without irradiation; (Group 5) SN38/Gd&Yb-LDH (200 μ L, 3 mg/kg for the dose of SN38) with irradiation; (Group 6) SN38&ICG (200 μ L, 3 mg/kg for the total dose of SN38 and ICG) without irradiation; (Group 7) ICG/Gd&Yb-LDH (200 μ L, 3 mg/kg for the dose of ICG) with irradiation; (Group 8) SN38&ICG/Gd&Yb-LDH (200 μ L, 3 mg/kg for the total dose of SN38 and ICG) with irradiation. The irradiation was carried out at 1.0 W/cm² for 3 min. The tumor size was measured by a caliper every two days with 16 days' treatment, and the volume was calculated as:

$$Volume = tumor\ length \times tumor\ width^2 \times 0.5 \quad (6)$$

Relative tumor volume was calculated as V/V_0 (V and V_0 are the tumor volume measured at

time t and t_0 , respectively).

Histology examination. On day 16, the mice were euthanized, and tumors as well as main organs were collected and fixed in 4% formalin for histology analysis. All the tissues were sliced to 3–5 mm for hematoxylin and eosin (H&E) staining and examined by a digital microscope (Leica).

Computational methods. The geometry optimizations of SN38 and ICG were performed at Gaussian09¹ software package with PM6² semiempirical method. According to the ratio of atoms in the unit cell, Mg: Al: Gd: Yb= 2: 0.8: 0.1: 0.1, we employed 3×1 supercell as the initial model. Taking into account the optimal loading rate for Gd&Yb-LDH, six ICG and twenty SN38 molecules are included in the modeling system. The solvent is explicit water molecules with a density of 1 g/cm³. We selected the last snapshot to analyze hydrogen bond interactions.

The process of anneal and dynamics were performed using Forcite module in Materials Studio (MS)³ software with Universal Force Field (UFF)⁴. The temperature and pressure were controlled using the Andersen and Berendsen method, respectively. The long-range coulombic interactions were computed by the Ewald summation technique, and the van der Waals interactions were calculated using the “spline-cutoff” method. The MD time step was set to 1 fs. 10 ps simulated annealing was taken to obtain stable structures of the complexes at the experimental temperatures in isothermal-isobaric ensemble. At 298.15K, 310.15K, 318.15K, 323.15K and 328.15K, 9 ns molecular dynamics simulations were carried out at a pressure of 1 bar, respectively.

Diffusivity coefficient was calculated by the mean square displacement (MSD) of ICG and

SN38 by Eq. (7)⁵:

$$D = \frac{1}{6} \lim_{t \rightarrow \infty} \frac{d}{dt} \sum_{i=1}^N ([r_i(t) - r_0(0)]^2) \quad (7)$$

where D is diffusion coefficient; $r_i(t)$ is the location of particle i at time t ; $r_0(0)$ represents the initial position.

Statistical analysis. Data were expressed as mean \pm standard deviation. The significant differences among groups were determined using one-way ANOVA analysis followed by Tukey's post-test: (*) $P < 0.05$, (**) $P < 0.01$ and (***) $P < 0.001$.

Sample characterization. Shimadzu XRD-6000 diffractometer with a Cu $K\alpha$ source was used to recorded powder X-ray diffraction patterns, with a scan step of 0.02° and a scan range between 3° and 70° . For colloid LDH samples, XRD tests were performed by dripping a droplet of colloid LDH sample onto a silicon wafer, which was then covered by a PET film. In addition, the control sample was obtained by drying the above colloid LDH sample on silicon wafer. The morphology of samples was investigated using high resolution transmission electron microscope (HRTEM) images with JEOL, JEM-2100 in the accelerating voltage of 200 kV. Inductively coupled plasma (ICP) emission spectroscopy was used to determine the chemical composition of Gd&Yb-LDH samples on a Shimadzu ICPS-7500 instrument. The particle size distribution was analyzed by a Malvern Mastersizer 2000 laser particle size analyzer. Fourier transform infrared (FT-IR) spectra were recorded from 3200 to 400 cm^{-1} in 2 cm^{-1} resolutions on a Vector 22 (Bruker) spectrophotometer. Shimadzu U-3000 spectrophotometer, with a slit width of 1.0 nm , was applied to record UV-vis-NIR absorption spectra from 300 to 900 nm . The fluorescence spectra were collected on a RF-5301PC fluorospectrophotometer (excitation wavelength of 370 nm) from 400 to

720 nm, and the width of both excitation and emission slit was 3 nm. Isothermal titration calorimetry (ITC) measurements were performed on a Nano ITC (TA Instruments Waters, LLC, UT). Temperature detection and thermal infrared images were recorded by a thermal infrared imaging camera (Fluke Ti450, USA). Fluorescence images were obtained on a Leica confocal laser scanning microscopy (Leica TCS SP5, Germany). *In vitro* cellular fluorescence quantity was performed on a flow cytometer (MoFlo XDP, Beckman Coulter). *In vivo* NIRF images were obtained using an IVIS Lumina fluorescence imaging system. The MRI experiments were conducted on a Bruker PharmaScan device (7 T). CT measurements were performed on SIEMENS Inveon device (Germany). An automated hematology analyzer (Bayer Advia 2120) and automatic biochemical analyzer (Olympus AU400) were used for blood cell counts and serum biochemistry analysis, respectively.

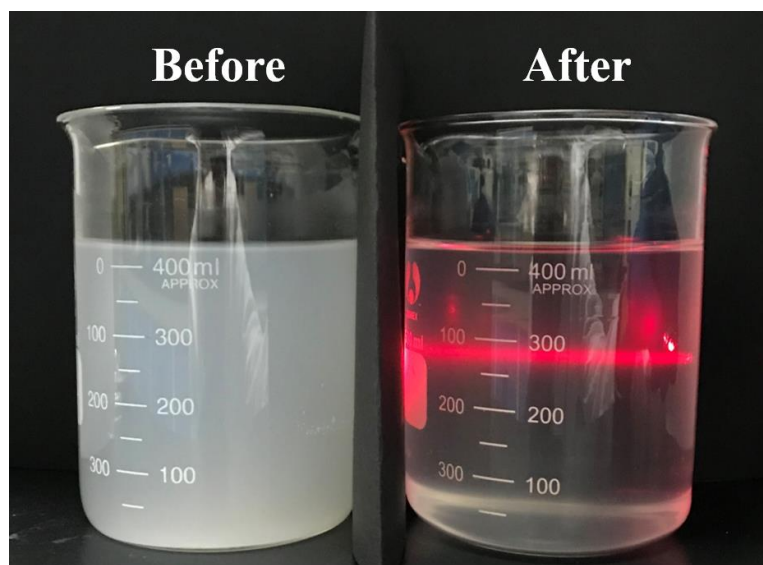


Figure S1. Digital photographs of the as-prepared Gd&Yb-LDH nanosheets suspension before and after 4000 rps centrifugation.

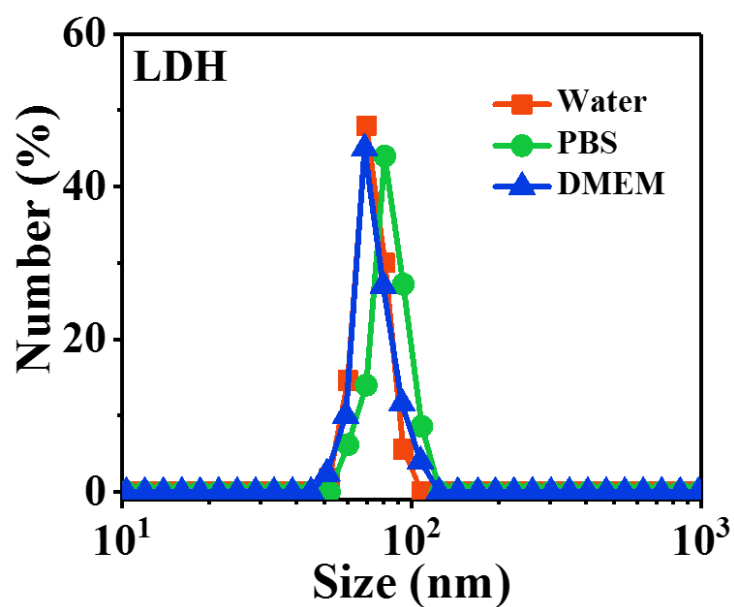


Figure S2. Size distribution of Gd&Yb-LDH nanosheets in water, PBS and DMEM culture medium, respectively.

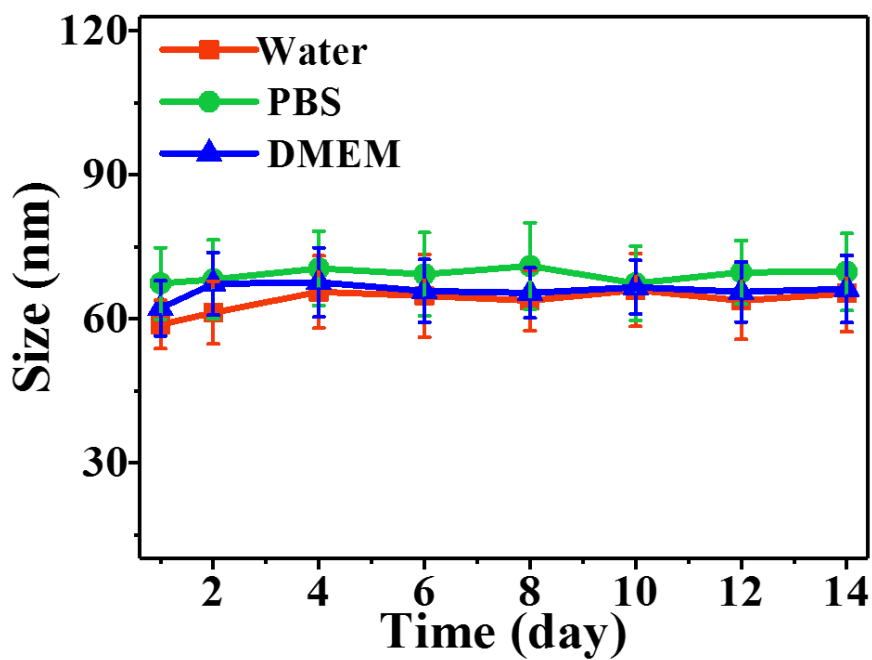


Figure S3. Particle size of Gd&Yb-LDH in water, PBS or DMEM for 14 days.

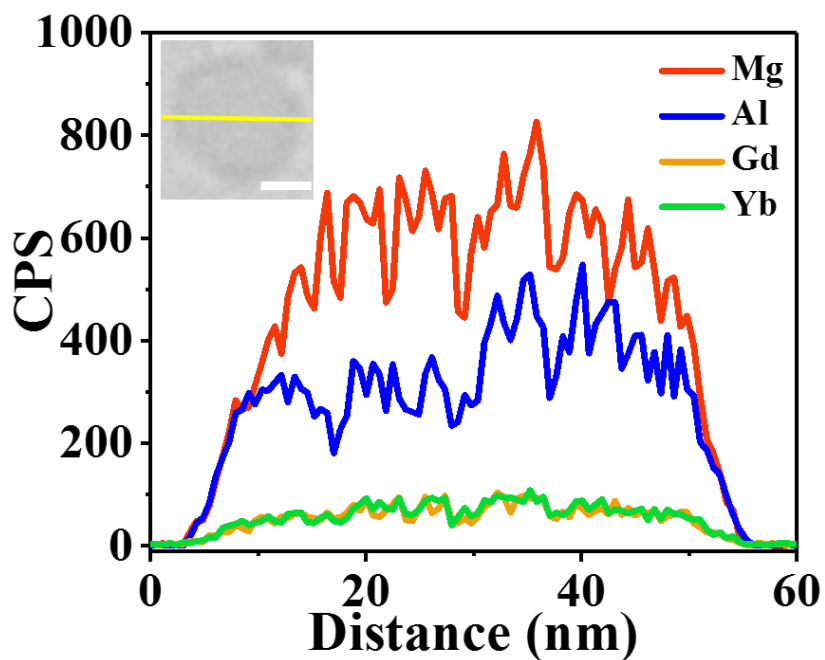


Figure S4. Elemental EDX line profiles of Gd&Yb-LDH nanosheets for Mg, Al, Yb and Gd, respectively. Scale bar: 20 nm.

Table S1. Comparison study on loading capacity (LC) of SN38 by various drug carriers

Therapeutic Agent	Drug Carrier	Loading Capacity-1 ^a	Loading Capacity-2 ^b	Refs
SN38	Gd&Yb-LDH	925%	90.2%	This work
SN38	MoS ₂	118%		<i>Adv. Mater.</i> , 2014 , 26, 3433
SN38	MCM-41	25%		<i>J. Phys. Chem. B</i> , 2010 , 114, 5903
SN38	CSPT NPs	18%		<i>Biomater. Sci.</i> , 2015 , 3, 1061
SN38	Graphene oxide	16.7%		<i>J. Photoch. Photobio. B.</i> , 2014 , 135, 7
SN38	PEGylated graphene oxide	15%		<i>J. Am. Chem. Soc.</i> , 2008 , 130, 10876
CPT	Ac-KK(CPT)-NH ₂ dipeptide	47%		<i>Chem. Eur. J.</i> , 2015 , 21, 101
DTX-SN38	Heterodimeric prodrugs		92.3%	<i>Theranostics</i> , 2017 , 7, 3638
SN38	Self-assembled Lipophilic tail		78.8%	<i>Adv. Funct. Mater.</i> , 2015 , 25, 4956
SN38	P-1-4 polymer		11.5%	<i>J. Controlled Release</i> , 2010 , 144, 314
SN38	PEG- PLA		5%	<i>Angew. Chem. Int. Edit.</i> , 2014 , 126, 11716
SN38	polymer		0.1%	<i>Angew. Chem. Int. Edit.</i> , 2016 , 128, 2846
CTX	Self-assembled nanomedicines		69.3	<i>Cancer Res.</i> , 2017 , 77, 6967
CPT	OEG-CPT		58%	<i>J. Am. Chem. Soc.</i> , 2010 , 132, 4259

^aLC-1 = $(W_{Fed} - W_{Non-encapsulated}) / W_{Gd\&Yb-LDH} \times 100\%$, ^bLC-2 = $(W_{Fed} - W_{Non-encapsulated}) / W_{total} \times 100\%$, where W_{Fed} represents the initial total mass of added drug; $W_{Non-encapsulated}$ is the unencapsulated drug mass in supernatant after centrifugation; $W_{Gd\&Yb-LDH}$ represents the total mass of added Gd&Yb-LDH during the drug loading; W_{total} represents the total mass of added Gd&Yb-LDH and encapsulated drug.

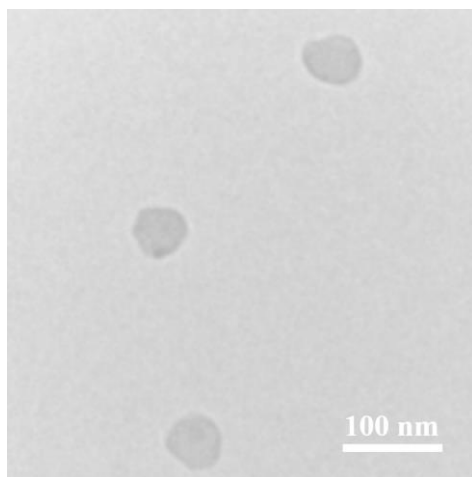


Figure S5. HRTEM image of SN38&ICG/Gd&Yb-LDH nanosheet.

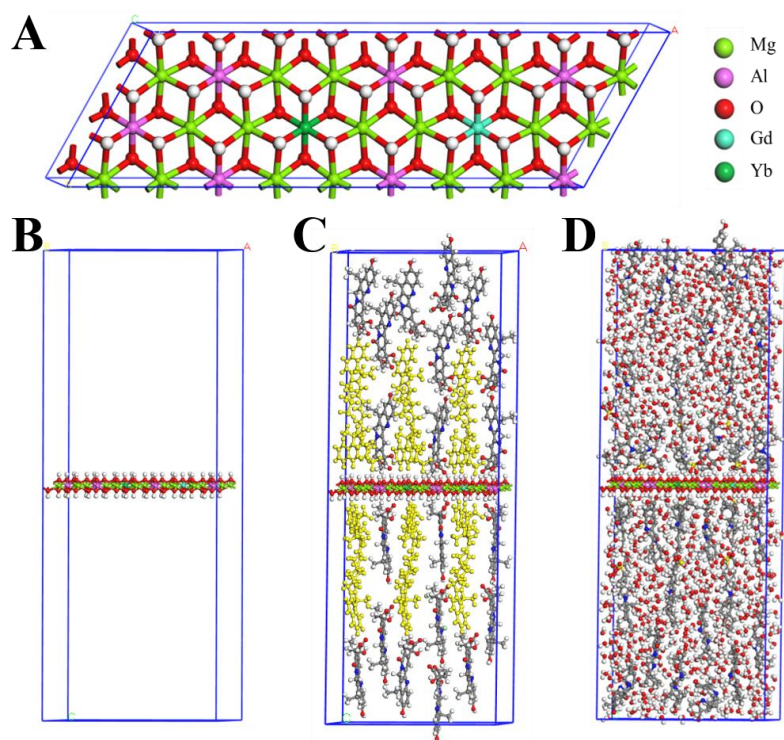


Figure S6. The specific process of modeling. Top view (A) and side view (B) of Gd&Yb-LDH (Mg: Al: Gd: Yb= 2: 0.8: 0.1: 0.1). (C) Six ICG and twenty SN38 molecules are introduced in the system for the simulation of optimum loading rate. (D) Explicit water molecules (density: 1 g/cm³) are added as the solvent environment.

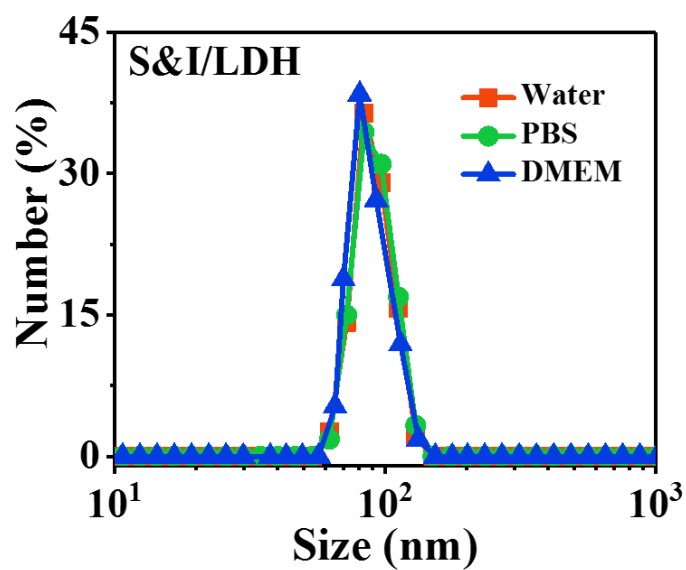


Figure S7. Size distribution of SN38&ICG/Gd&Yb-LDH in water, PBS and DMEM culture medium, respectively.

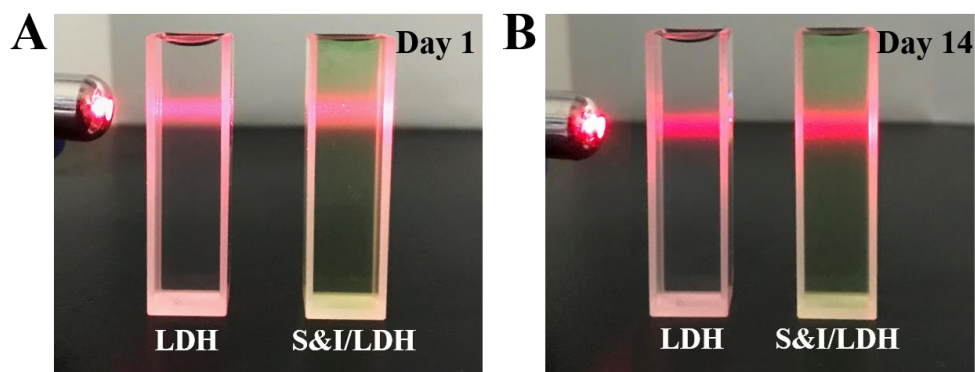


Figure S8. Tyndall effect of Gd&Yb-LDH and SN38&ICG/Gd&Yb-LDH in aqueous suspension at day 1 and day 14, respectively.

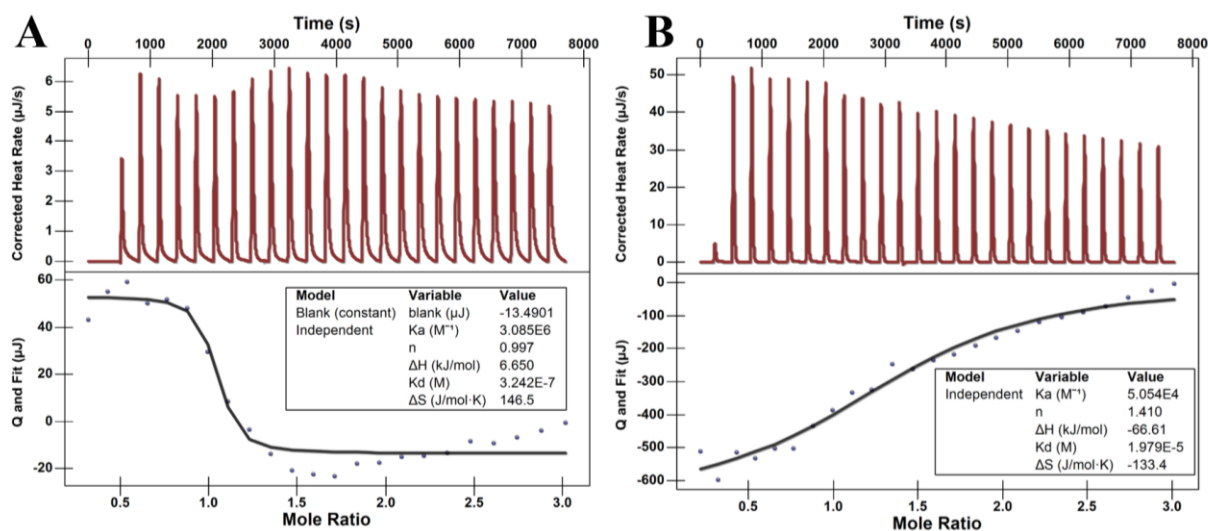


Figure S9. (A) ITC titration measurements of SN38 (1.0×10^{-4} mol/L) and ICG (1.0×10^{-3} mol/L); (B) ITC titration measurements of SN38&ICG (1.0×10^{-4} mol/L) and Gd&Yb-LDH (1.0×10^{-3} mol/L).

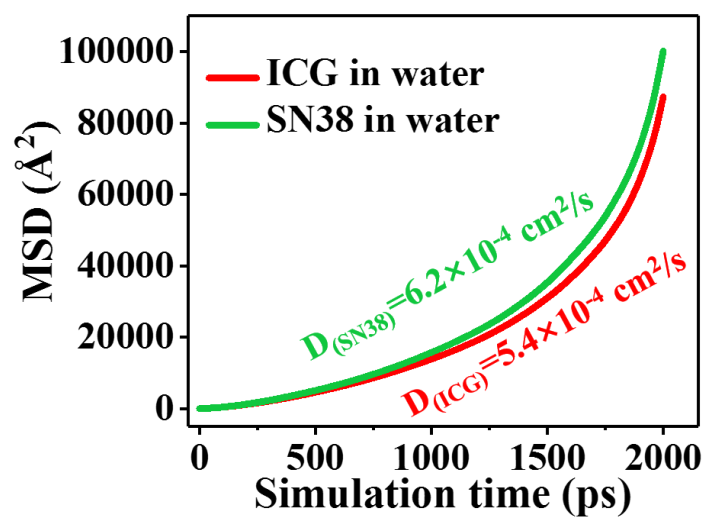


Figure S10. Mean squared displacement of ICG and SN38 in water within 2 ns molecular dynamics simulations at 298.15 K.

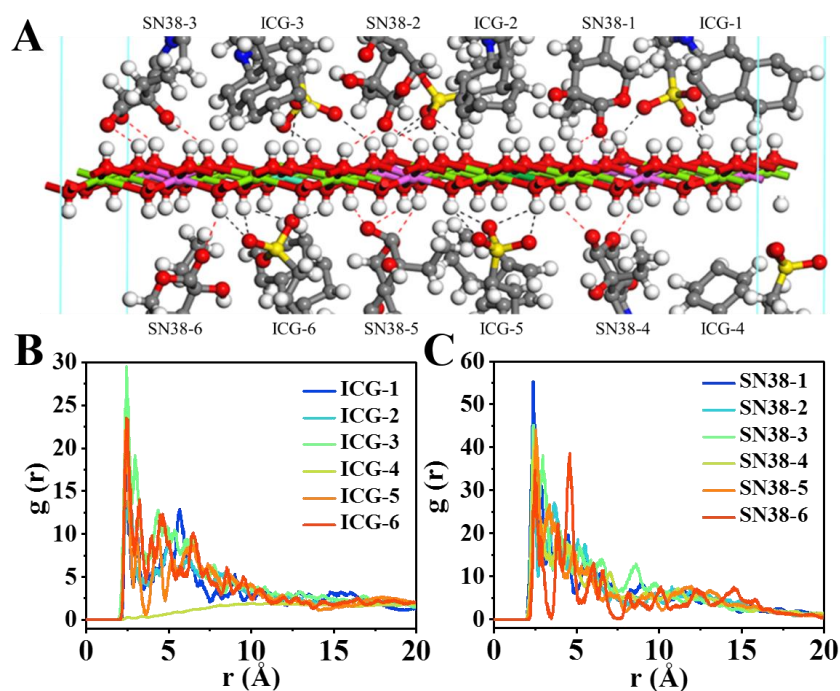


Figure S11. (A) Hydrogen bond between ICG, SN38 molecules and Gd&Yb-LDH monolayer. The red line represents the hydrogen bond formed by SN38 and Gd&Yb-LDH; the black line represents the hydrogen bond formed by ICG and Gd&Yb-LDH. (B) and (C) show the radial distribution function of ICG and SN38, respectively.

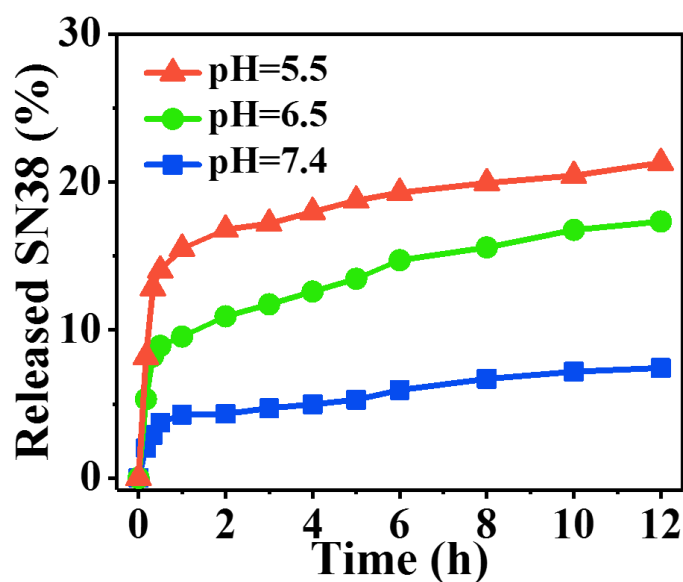


Figure S12. Release profiles of SN38 from SN38&ICG/Gd&Yb-LDH at pH 7.4, 6.5 and 5.5 for 12 h, respectively.

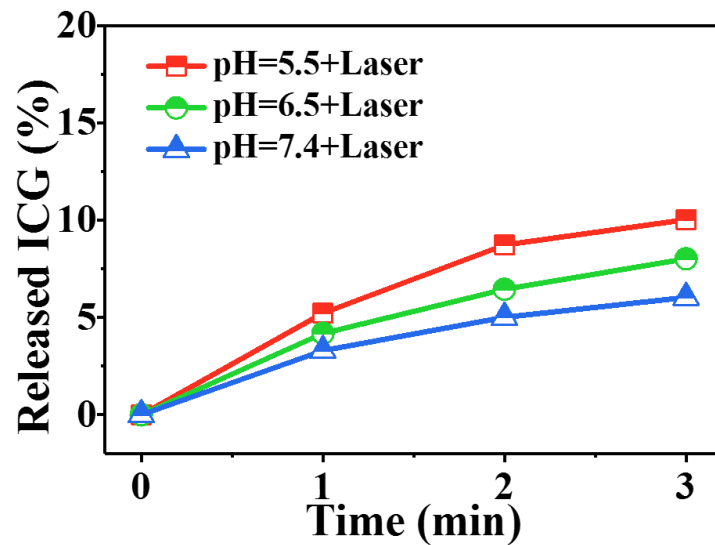


Figure S13. Release curves of ICG from SN38&ICG/Gd&Yb-LDH in PBS with 808 nm irradiation at pH 5.5, 6.5 and 7.4 (1.0 W/cm^2), respectively.

Table S2. Diffusion coefficient values of SN38 at selected temperatures

Temperature (K)	Diffusion coefficient (cm^2/s)
298.15	0.5×10^{-8}
310.15	3.0×10^{-8}
318.15	4.8×10^{-8}
323.15	5.3×10^{-8}
328.15	10.5×10^{-8}

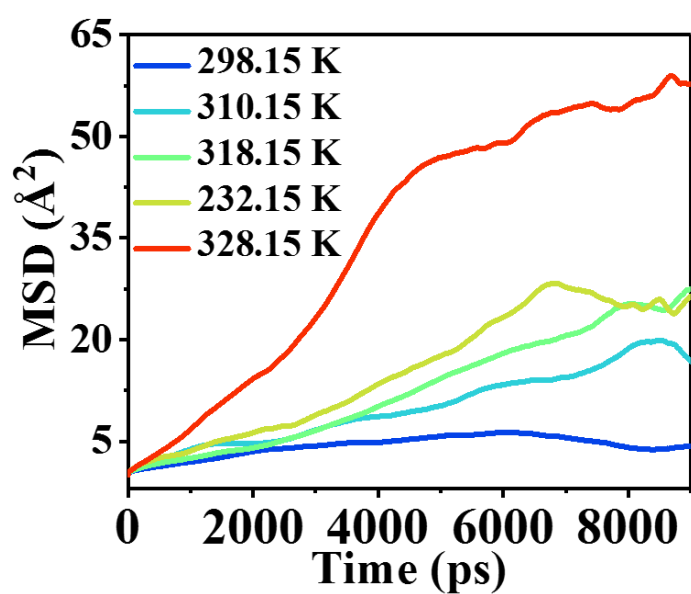


Figure S14. Mean squared displacement (MSD) of SN38 molecule at various temperatures within 9 ns molecular dynamics simulations. The MSD values in this figure are the average MSD value of six SN38 molecules.

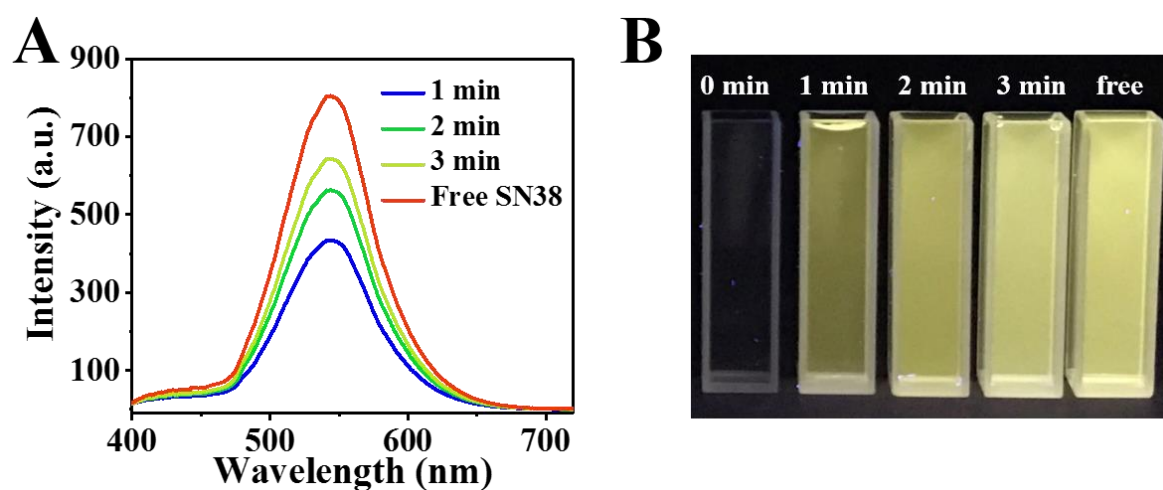


Figure S15. (A) Fluorescence intensity and corresponding photographs for free SN38 solution (5 $\mu\text{g}/\text{mL}$) and the supernatant of SN38&ICG/Gd&Yb-LDH after laser irradiation (808 nm, 1.0 W/cm^2) for 0 min, 1 min, 2 min and 3 min, respectively.

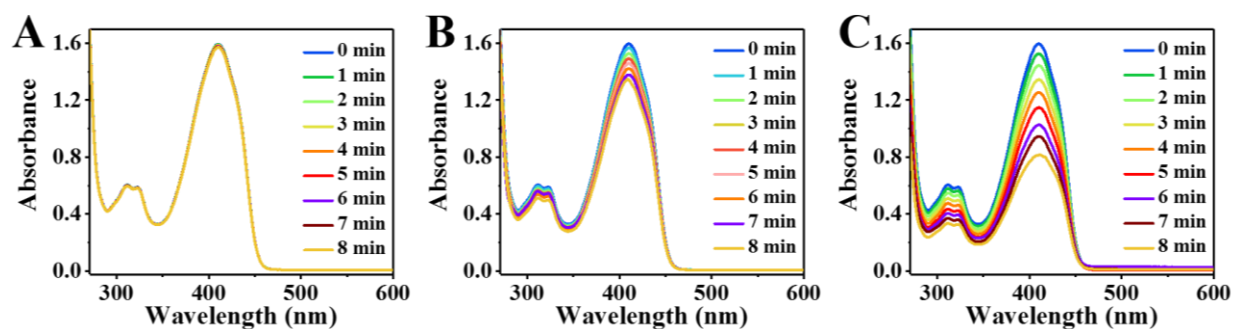


Figure S16. Decay curves of DPBF in the presence of (A) blank, (B) ICG, (C) SN38&ICG/Gd&Yb-LDH as a function of irradiation time (808 nm, 1.0 W/cm²).

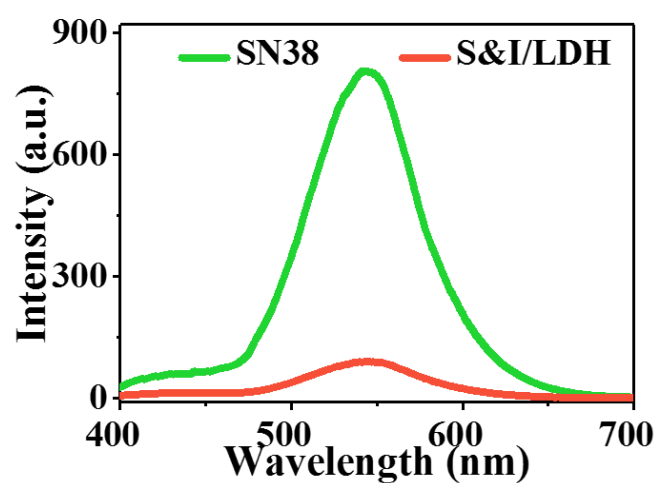


Figure S17. Fluorescence spectra of SN38 and SN38&ICG/Gd&Yb-LDH, respectively.

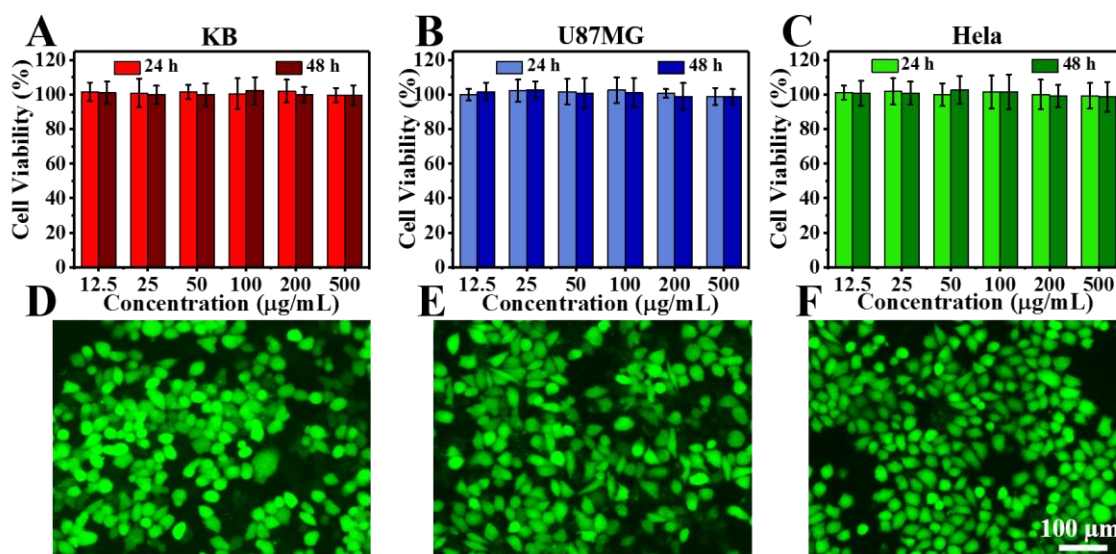


Figure S18. (A-C) Cell viability of KB, U87MG and HeLa cells incubated with various concentrations of Gd&Yb-LDH nanosheets. (D-F) Calcein-AM/PI staining of KB, U87MG and HeLa cells incubated with 500 µg/mL of Gd&Yb-LDH nanosheets.

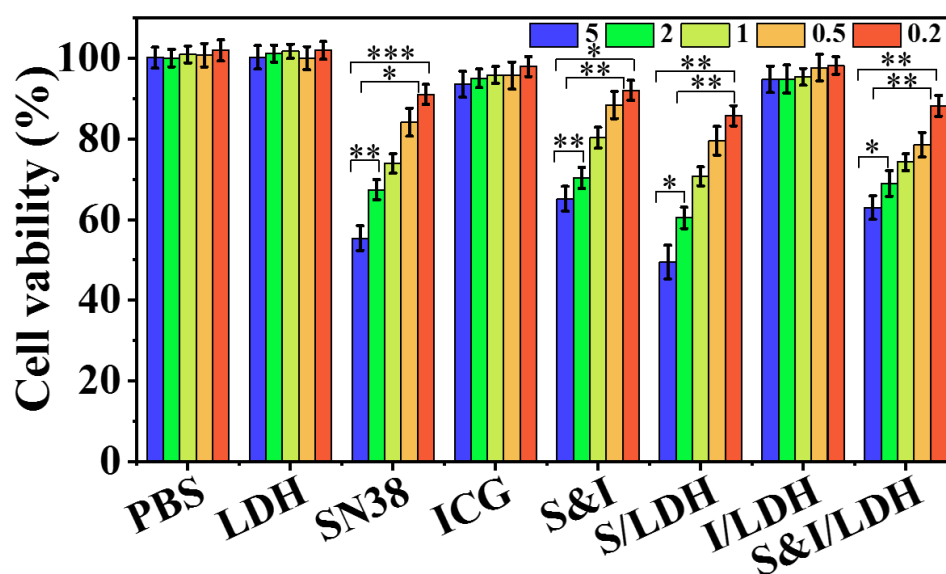


Figure S19. Viability of HeLa cells after treated with various concentrations of drug without NIR laser irradiation. P values in were calculated by Tukey's post-test (***) $P < 0.001$, (** $P < 0.01$, or * $P < 0.05$).

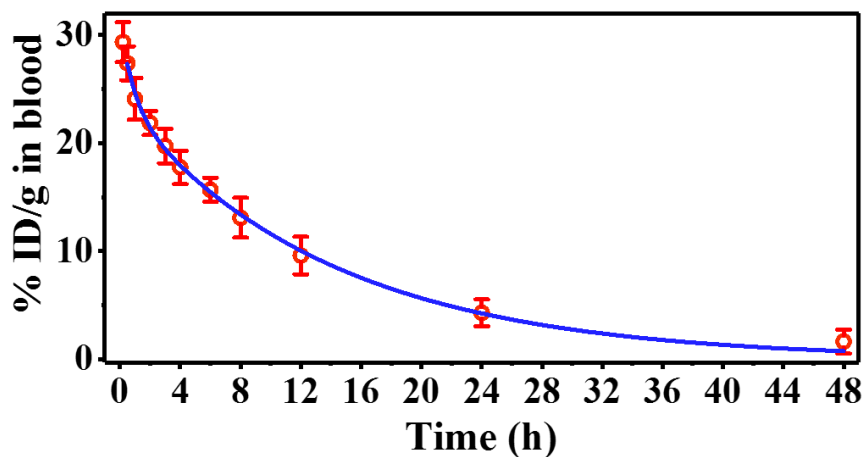


Figure S20. Blood circulation curve of SN38&ICG/Gd&Yb-LDH determined by Gd concentration in the blood of mice at different time points post-injection. The pharmacokinetics obeys a typical two compartment model.

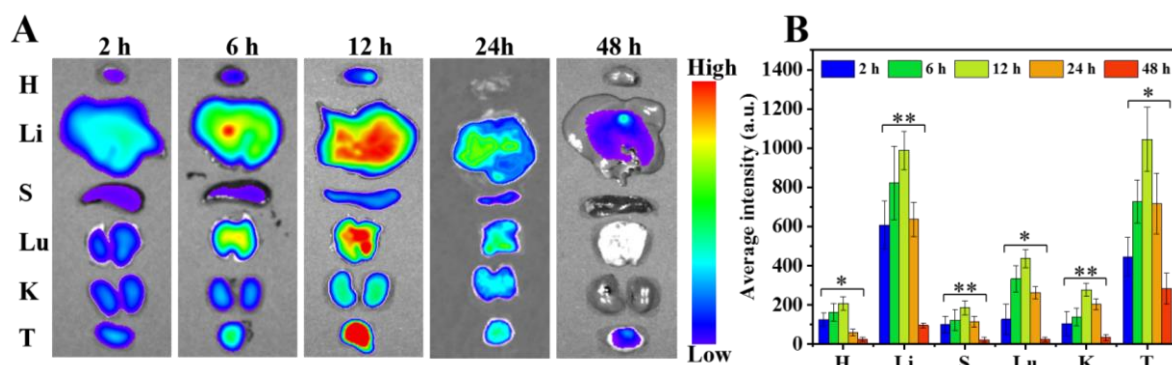


Figure S21. (A) *Ex vivo* fluorescence images of major organs at 2 h, 6 h, 12 h, 24 h and 48 h after intravenous injection of SN38&ICG/Gd&Yb-LDH. (B) Semiquantitative biodistribution of Ce6&AuNCs/Gd-LDH in nude mice determined by the averaged fluorescence intensity of each organ. The data are shown as mean \pm SD ($n = 6$); a single asterisk (*) indicates $P < 0.05$, and a double asterisk (**) indicates $P < 0.01$.

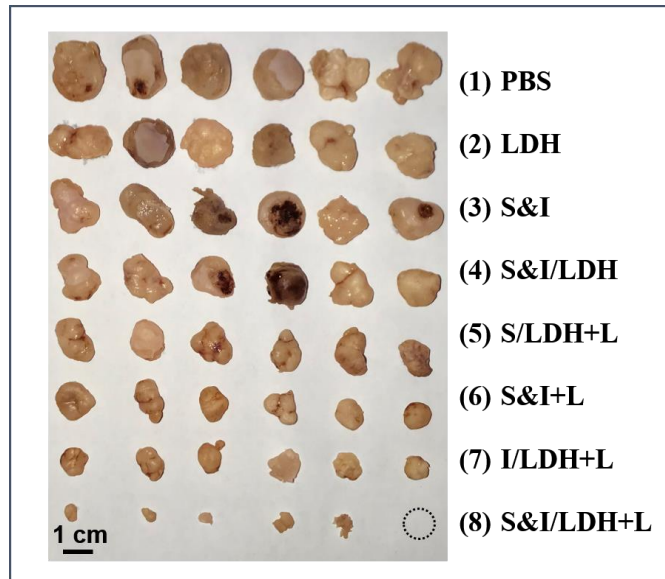


Figure S22. Digital photographs of excised tumors on day 16 after various treatments.

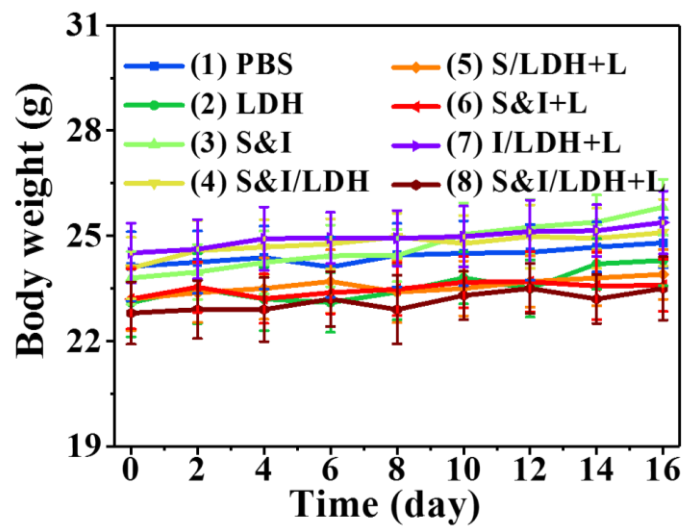


Figure S23. Body weight change of HeLa tumor bearing mice after various treatments as a function of time.

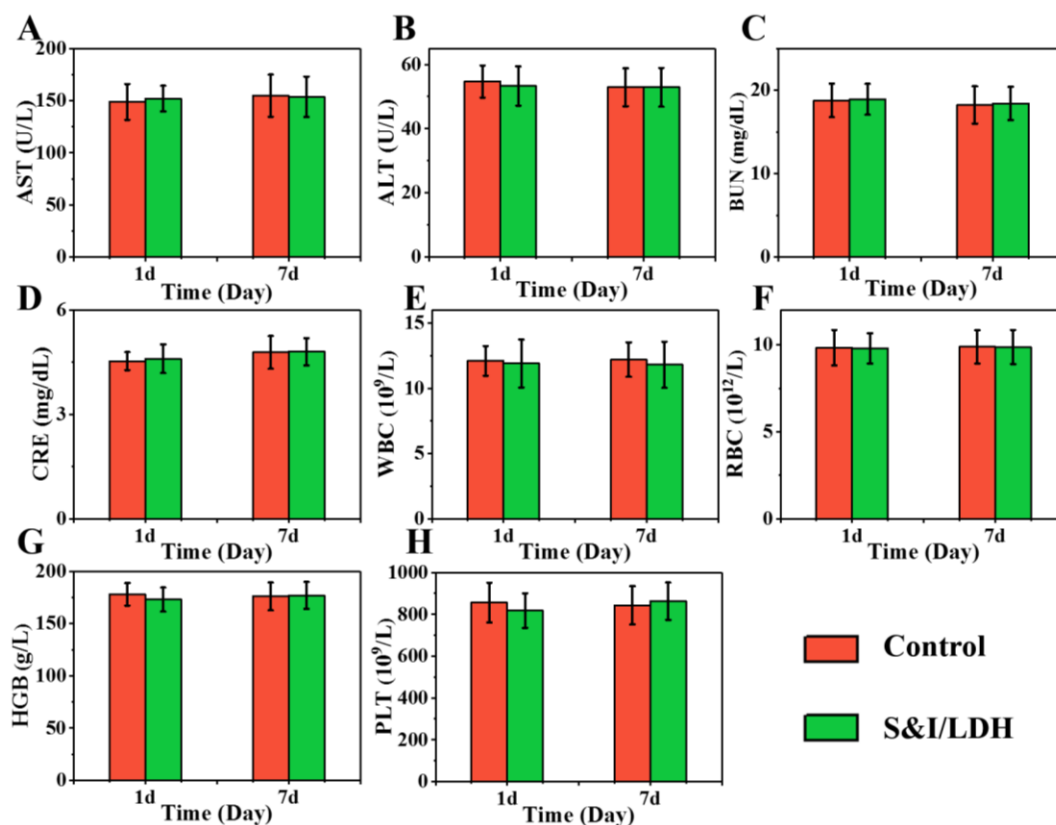


Figure S24. Kidney, liver function markers and blood cell counts of the nude mice bearing Hela tumors were detected after injection of saline (control) and SN38&ICG/Gd&Yb-LDH at Day 1 and Day 7, respectively.

References

- [1] F. Ponthan, M. Wickström, H. Gleissman, O. M. Fuskevåg, L. Segerström, B. Sveinbjörnsson, C. P. F. Redfern, S. Eksborg, P. Kogner and J. I. Johnsen, *Clin. Cancer Res.*, 2007, **13**, 1036.
- [2] S. H. Liu, Y. B. Guo, R. Q. Huang, J. F. Li, S. X. Huang, Y. Y. Kuang, L. Han and C. Jiang. *Biomaterials*, 2012, **33**, 4907.
- [3] M. J. Frisch, et al. Gaussian 09, Revision C.01, Gaussian Inc, 2009.
- [4] J. J. P. Stewart, *J. Mol. Model.*, 2007, **13**, 1173.
- [5] Accelrys Software. Materials Studio 8.0. Accelrys Software Inc, San Diego, 2014.
- [6] (a) A. K. Rappe, K. S. Colwell and C. J. Casewit, *J. Inorg. Chem.*, 1993, **32**, 3438; (b) A. K. Rappe, C. J. Casewit, K. S. Colwell, W. A. Goddard and W. M. Skiff, *J. Am. Chem. Soc.*, 1992, **114**, 10024; (c) A. K. Rappe, C. J. Casewit, K. S. Colwell, W. A. Goddard and W. M. Skiff, *J. Am. Chem. Soc.*, 1992, **114**, 10035; (d) C. J. Casewit, K. S. Colwell and A. K. Rappe, *J. Am. Chem. Soc.*, 1992, **114**, 10046.
- [7] L. Chen, Y.-L. He and W.-Q. Tao, *Numer. Heat. Tr.*, 2014, **65**, 216.